

PS-Net: Deep Partially Separable Modelling for Dynamic Magnetic Resonance Imaging

Chentao Cao, Zhuo-Xu Cui, Qingyong Zhu, Dong Liang, *Senior Member, IEEE*, Yanjie Zhu, *Member, IEEE*

Abstract—Deep learning methods driven by the low-rank regularization have achieved attractive performance in dynamic magnetic resonance (MR) imaging. However, most of these methods represent low-rank prior by hand-crafted nuclear norm, which cannot accurately approximate the low-rank prior over the entire dataset through a fixed regularization parameter. In this paper, we propose a learned low-rank method for dynamic MR imaging. In particular, we unrolled the semi-quadratic splitting method (HQS) algorithm for the partially separable (PS) model to a network, in which the low-rank is adaptively characterized by a learnable null-space transform. Experiments on the cardiac cine dataset show that the proposed model outperforms the state-of-the-art compressed sensing (CS) methods and existing deep learning methods both quantitatively and qualitatively.

Index Terms—Dynamic magnetic resonance imaging, Deep learning, Image reconstruction, Partially Separable, Annihilation

I. INTRODUCTION

DYNAMIC magnetic resonance imaging (MRI) plays a vital role in cardiac imaging because it can reveal information in spatial anatomy and temporal motion dimensions. However, the inherent long scan time of MRI limits its spatial and temporal resolutions. Therefore, fast dynamic MRI via highly undersampling k-space data generates great research interest.

With the rise of deep learning, many deep learning-based fast MRI methods have been developed and shown promising results. These methods can be roughly divided into two categories: the end-to-end methods [1]–[4] and the unrolling-based methods [5] [6]. The end-to-end methods directly learn the mapping from the undersampled k-space data or image to the fully sampled one with a neural network. It usually requires a large amount of training data and takes a long training time [7] [8], and has weak interpretability. The unrolling-based methods unroll the iterative solving step of the compressed sensing (CS) model into a neural network, which learns the regularization parameters, sparsifying transforms, etc. in the

This work was supported by the National Key Research and Development Program of China under Grant 2020YFA0712200.

Corresponding author: yj.zhu@siat.ac.cn (Yanjie Zhu)

Chentao Cao and Zhuo-Xu Cui contributed equally to this manuscript

Chentao Cao and Yanjie Zhu are with Lauterbur Research Center for Biomedical Imaging, Shenzhen Institutes of Advanced Technology, Chinese Academy of Sciences, Shenzhen, China

Chentao Cao is also with University of Chinese Academy of Sciences, Beijing, China

Yanjie Zhu is also with National Center for Applied Mathematics Shenzhen (NCAMS), Shenzhen, China

Zhuo-Xu Cui, Qingyong Zhu, and Dong Liang are with Research Center for Medical AI, Shenzhen Institutes of Advanced Technology, Chinese Academy of Sciences, Shenzhen, China

model. Compared with the end-to-end methods, unrolling-based methods are more prevalent in the MR reconstruction field [9]–[11] since it requires less training data and lower computing power of graphics cards.

Several unrolling-based methods have been proposed for fast dynamic MRI [12]–[14]. Most of them employ low-rank prior to characterize the correlations among image frames. Low-rank prior is often approximated via the nuclear norm minimization, which is solved by the singular value soft threshold (SVT) with a hand-crafted cutoff parameter. When unrolled into a network, it's straightforward to learn the optimized cutoff parameter of SVT, i.e., the threshold, instead of empirical choosing. However, SVT loses small components and may cause image blurring. In addition, due to its limited representation ability of low-rank and only relaxing low degree of freedom for learning cutoff parameters, these SVT-learning based methods result in inadequate characterization of the image low-rank even if the threshold is optimized through learning. In the case of highly accelerated cardiac dynamic imaging, the unrolling-based methods with this type of learnable low-rank are prone to suffer from aliasing artifacts, especially in systole. Another way of unrolling methods is learning the nonlinear transforms in CS via the network to more effectively sparsify images. Since the transforms are adaptively learned, the resulting sparse representation is more accurate than the fixed-base transforms. Inspired by this, a learnable low-rank representation may also enhance the low rankness of the image than the nuclear norm.

In this paper, we proposed a partially separable network (PS-Net) to more adaptively characterize the low-rank prior through a learnable null space transform. More specifically, since dynamic MRI can be represented in a partially separable (PS) form [15], a null space filter can be used to annihilate the PS model according to the classical Prony's results [16]. Then, the low rankness can be implicitly characterized by an adaptively learned null space transform. We combined this low-rank constrain with a sparse constrain under the framework of compressed sensing. The corresponding optimization problem was solved in an iterative form with the semi-quadratic splitting method (HQS). The iterative steps were unrolled into a network dubbed PS-Net. All the regularization parameters and null space transform are set as learnable in the PS-Net. Our contribution can be summarized as follows:

- 1) The low rankness of dynamic MRI is first represented by a learnable null space transform, which is more adaptive and accurate than the nuclear norm representation.
- 2) Different from previous learnable transform methods, the null space transform in the PS-Net can be formulated

as a Hankel matrix multiplication, which is equivalent to the convolution operation and can be naturally unrolled into a convolutional network module.

3) The reconstruction quality of our proposed method is better than the state-of-the-art methods and does not alias adjacent image frames at a high acceleration rate.

II. METHODS

A. Problem formulation

The task of dynamic MRI reconstruction is to reconstruct MRI images $\gamma \in \mathbb{C}^{N_x N_y N_t}$ from undersampled raw k-space data $y \in \mathbb{C}^{N_x N_y N_t}$. Here, N_x and N_y represent the image size and N_t represents the number of time frames. This task is generally solved by the following unconstrained optimization problem:

$$\gamma^* = \arg \min_{\gamma} \frac{1}{2} \|MF\gamma - y\|_F^2 + R(\gamma) \quad (1)$$

where F is the Fourier operator, M is the undersampling operator, and $R(\gamma)$ is the prior regularization term. In this letter, we use the sparse prior and subspace model as the prior regularization term.

1) *The sparse prior*: Since the intensities of adjacent pixels in MR images are similar to each other, the gradient of the image domain satisfies the sparse property and thus satisfies the annihilation relationship [17]: $(\nabla\gamma)\mu = 0$, where γ is the image and μ is a set of bandlimited functions. According to the equivalence of convolution and Hankel matrix product, we can get: $H(\widehat{\nabla\gamma})h_s = 0$, where $\widehat{\nabla\gamma}$ represents the Fourier coefficients of the gradient of γ , $H(\widehat{\nabla\gamma})$ is the Hankel-structured matrix in the $N_x N_y$ direction and h_s is the Fourier transform of μ .

2) *Subspace Model*: Subspace models have been used to solve dynamic magnetic resonance imaging problems over the past decade, including the partially separable model [15]:

$$\gamma(r, t) = \sum_{l=1}^L c_l(r) \phi_l(t) \quad (2)$$

where $\phi_l(t)$ is a set of time bases, $c_l(r)$ is the corresponding space base, and $\gamma(r, t)$ is the dynamic magnetic resonance image to be reconstructed, $\gamma \in \mathbb{C}^{N_x N_y N_t}$. The classical Prony's results [16] rely on the annihilation of such model by

$$h_{ps}(t, z) = \prod_{l=1}^L \left(1 - \phi_l(t)^{\frac{1}{z}} z^{-1} \right) \quad (3)$$

such that the associated L -tap filter $h_{ps}(t, z)$ annihilates the dynamic MRI PS model $\gamma(r, t)$:

$$(h_{ps} * \gamma)(r, t) = 0, \quad \forall r, t \quad (4)$$

By the equivalence relation of Hankel matrix and convolution, the above relation is equivalent to: $H(\gamma)h_{ps} = 0$. Here $H(\gamma)$ is a linear convolution matrix with Hankel-structure in the N_t direction. The above annihilation relation indirectly characterizes the low-rank via the null space filter.

B. The proposed method: PS Network for Dynamic MRI

With the above subspace model and sparse priors, we can formulate the dynamic MRI reconstruction problem as the following unconstrained two-norm minimization problem:

$$\arg \min_{\gamma} \frac{1}{2} \|MF\gamma - y\|_F^2 + \lambda_1 \|H_1(\widehat{\nabla\gamma})h_s\|_F^2 + \lambda_2 \|H_2(\gamma)h_{ps}\|_F^2 \quad (5)$$

where $\|H_1(\widehat{\nabla\gamma})h_s\|_F^2$ represents the sparse regularizer and $\|H_2(\gamma)h_{ps}\|_F^2$ is the null space annihilation regularizer, which is derived by the partially separable property. λ_1 and λ_2 are the corresponding regularization parameters. To solve the optimization problem in Eq. (5), we introduce two auxiliary variables \widehat{U} , Z . The reformed optimization problem is as follows:

$$\begin{aligned} \min_{\gamma, \widehat{U}, Z} & \frac{1}{2} \|MF\gamma - y\|_F^2 + \lambda_1 \|H_1(\widehat{U})h_s\|_F^2 + \lambda_2 \|H_2(Z)h_{ps}\|_F^2 \\ \text{s.t.} & \quad \widehat{U} = \widehat{\nabla\gamma}, \quad Z = \gamma \end{aligned} \quad (6)$$

Based on the semi-quadratic splitting method (HQS), we can construct an iterative solution algorithm for the above regularization model, and solve different subproblems according to different variables:

$$\begin{cases} \widehat{U}_k = \min_{\widehat{U}} \frac{\rho_1}{2} \left\| \widehat{U} - \begin{pmatrix} iw_x F(\gamma_{k-1}) \\ iw_y F(\gamma_{k-1}) \end{pmatrix} \right\|_F^2 \\ \quad + \lambda_1 \|H_1(\widehat{U})h_s\|_F^2 \\ Z_k = \min_Z \frac{\rho_2}{2} \|Z - \gamma_{k-1}\|_F^2 + \lambda_2 \|H_2(Z)h_{ps}\|_F^2 \\ \gamma_k = \min_{\gamma} \frac{\rho_1}{2} \left\| \widehat{U}_{k-1} - \begin{pmatrix} iw_x F(\gamma) \\ iw_y F(\gamma) \end{pmatrix} \right\|_F^2 \\ \quad + \frac{1}{2} \|MF\gamma - y\|_F^2 + \frac{\rho_2}{2} \|Z_{k-1} - \gamma\|_F^2 \end{cases} \quad (7)$$

where $\begin{pmatrix} iw_x F(\gamma) \\ iw_y F(\gamma) \end{pmatrix}$ is the mapping from γ to $\widehat{\nabla\gamma}$, and w_x and w_y denote the k-space coordinates: $\widehat{\nabla\gamma} = \begin{pmatrix} iw_x F(\gamma) \\ iw_y F(\gamma) \end{pmatrix}$.

To solve the above subproblems, we propose the unrolling Partially Separable network, dubbed PS-Net. The iterative steps of Eq. (7) are unrolling into iterative blocks of the network, each of which consists of three modules named sparse module \widehat{U}_k , PS annihilation module Z_k , and reconstruction module γ_k , as shown in Fig. 1.

- **The sparse module \widehat{U}_k** : From the annihilation relationship between the filter and k-space, we can use a residual 2D convolutional neural network to learn this set of filters, where the input is k-space data, and the convolution direction is along the $N_x N_y$ direction.
- **The PS annihilation module Z_k** : The PS annihilation layer characterizes the low-rank prior by a learnable null space filter mapping. The process of this mapping is learned through a 1D convolution layer along the time direction.
- **The reconstruction module γ_k** : In the update step of γ_k , ρ_1 and ρ_2 are set to be learnable to avoid the empirical problem of artificially tuning hyperparameters.

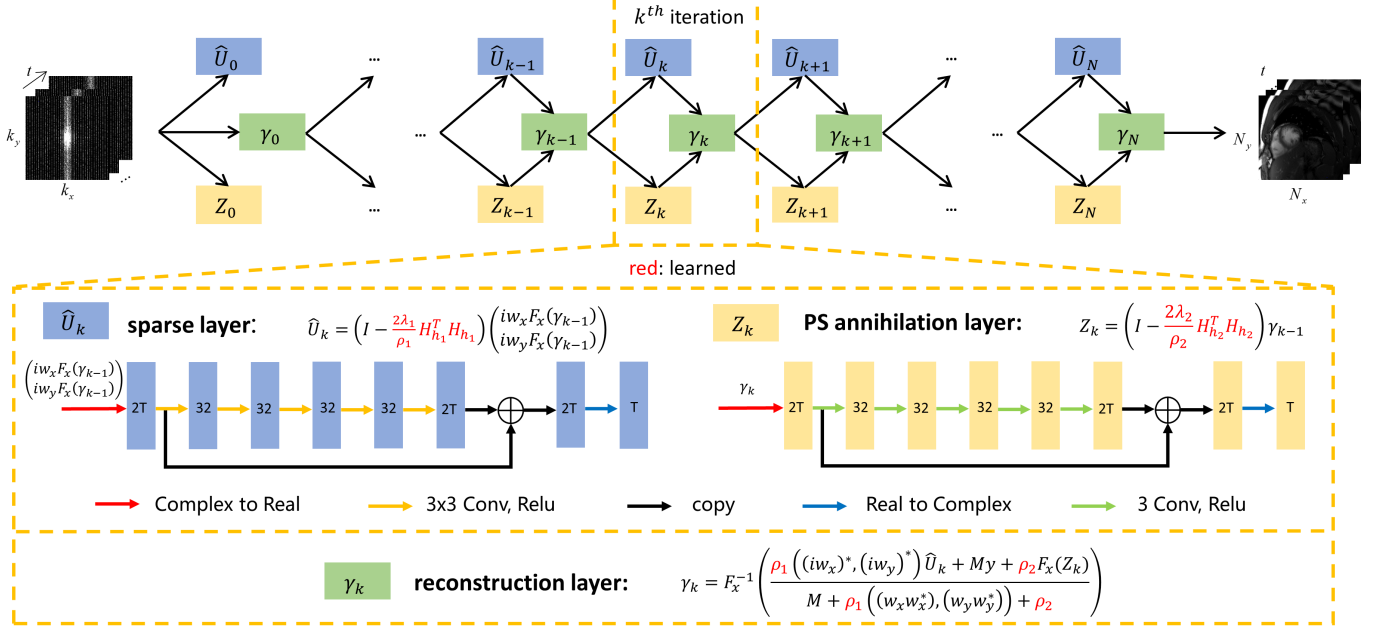


Fig. 1. The proposed PS-Net for dynamic MRI. PS-Net is defined over the iterative procedures of Eq. (7). The three procedures in Eq. (7) correspond to the three modules in PS-Net, which are named sparse module \hat{U}_k , L+SPS annihilation module Z_k and reconstruction module γ_k . T represents the size of the time dimension. H_{h_s} and $H_{h_{ps}}$ represent the Hankel-structured matrixes of h_s and h_{ps} .

These learnable parameters in PS-Net are all initialized to 1 and they are different among blocks. The input y is the undersampled k-space data and M is the undersampled mask. F is the 2D spatial Fourier operator.

III. EXPERIMENTS AND RESULTS

A. Dataset and Experimental Details

1) *Cardiac cine Dataset*: The fully sampled cardiac cine data were collected from 29 healthy volunteers on a 3T scanner (MAGNETOM Trio, Siemens Healthcare, Erlangen, Germany) with a 20-channel receiver coil. We randomly selected 25 volunteers for training and the rest for testing and we obtained 800 2D-t cardiac MR data of size $192 \times 192 \times 18$ ($x \times y \times t$) for training and 118 data values for testing. The raw multi-coil data of each frame were combined by the adaptive coil combining method [18] to produce single-coil complex-valued images.

To obtain training input-output pairs, we artificially apply an undersampling mask to the training data. We fully sampled the frequency encoding (along k_x) and randomly undersampled the phase encoding (along k_y) with a Cartesian mask [19].

2) *Model configuration*: The main structure of PS-Net is shown in Fig. 1. It is implemented with 10 iterative blocks and each block has 3 modules: sparse module, PS annihilation module, and reconstruction module. The sparse module is a 2D residual CNN with 5 convolution layers and each convolution layer consists of 32 3×3 filters. The PS annihilation module is a 1D residual CNN with 5 convolution layers and the size of the convolution kernel is 3. The number of convolution channels for the sparse module and PS annihilation module is 32. All the above convolution layers are followed by ReLU non-linearity [20]. Because the convolution is designed for

floating-point data and is incapable of handling complex data, We divide input data into $2T$ channels, where T represents the size of the time dimension.

PS-Net is trained to minimize the pixel-wise l_2 norm between the reconstructed image and the fully sampled image, given the training samples that undersampled k-space data as input and the corresponding fully sampled image as the ground truth. The batch size was 1. The exponential decay learning rate was used in the training procedure and the initial value was set to 0.001 with a decay of 0.95. The model was implemented using Tensorflow version 2.7 [21] with CUDA 11 and cuDNN support.

3) *Performance Evaluation*: Three metrics including the mean square error (MSE), peak signal to noise ratio (PSNR) and structural similarity index (SSIM) [22] were employed to analyze the reconstruction, where lower MSE, higher PSNR, and higher SSIM indicated better reconstruction. We compared PS-Net with the state-of-the-art dynamic MR methods with the compressed sensing approach L+S [23], the end-to-end approaches: DC-CNN [24], CRNN [25], and an unrolling approach: SLR-Net [12].

B. The reconstruction performance of the proposed PS-Net

The comparison between the PS-Net and the above-mentioned state-of-the-art methods at 8-fold acceleration is shown in Fig. 2. The error map in the third row shows that the image reconstructed using PS-Net appears much cleaner than other methods, indicating that our method achieves a better reconstruction effect. As can be seen from the y - t error maps, PS-Net is also more accurate in reconstruction in the time dimension. According to the quantitative evaluations in Table I, PS-Net achieves the best quantitative performance.

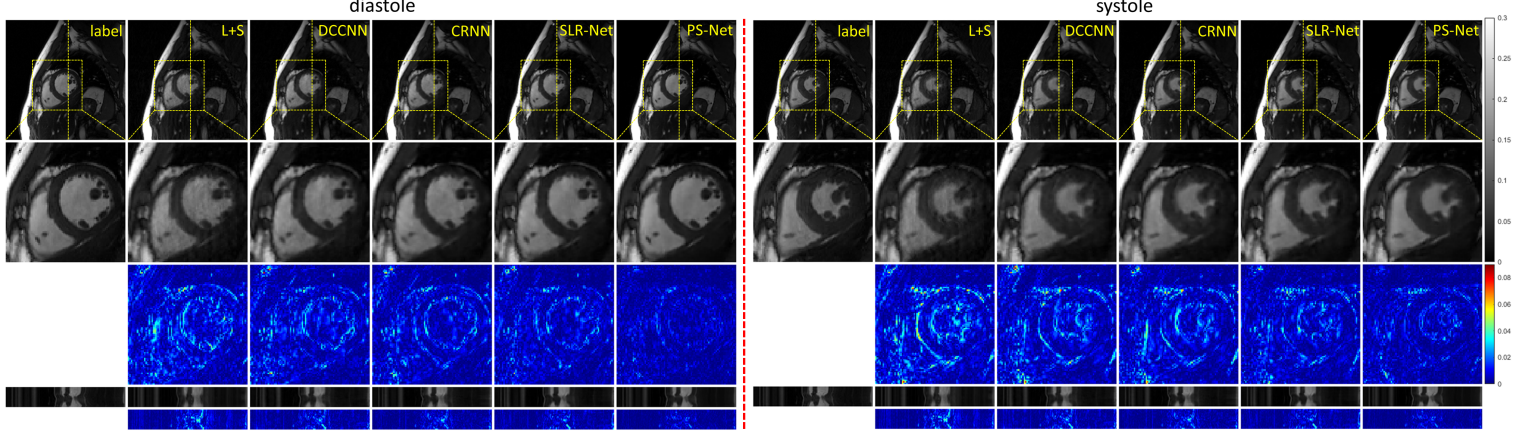


Fig. 2. The reconstruction results of the different methods (L+S, DC-CNN, CRNN, SLR-Net and the proposed PS-Net) at 8-fold acceleration on a single-coil cardiac cine dataset. The left side of the red dashed line is diastolic and the right side of the red dashed line is systolic. The first row shows the ground truth and the reconstruction results of these methods. The second row shows the enlarged views of their heart regions framed by a yellow box. The third row shows the error map (display range [0, 0.09]). The y-t image (extraction of the 92nd slice along the y and temporal dimensions) and the y-t image error are also given to show the reconstruction performance in the temporal dimension.

Both qualitative and quantitative results demonstrate that the proposed PS-Net can effectively explore the low-rank prior of dynamic data, thus improving the reconstruction performance.

We explored PS-Net's performance at higher acceleration in a single-coil scenario. The 10-fold, 12-fold, and 14-fold reconstruction results are shown in Fig. 3. The quantitative evaluations can be found in Table II. Our approach can still recover the image's dynamic content very well on such extremely undersampled data. Few artifacts at the extremely high acceleration rate indicate that the proposed method has great potential in ultra-fast dynamic imaging.

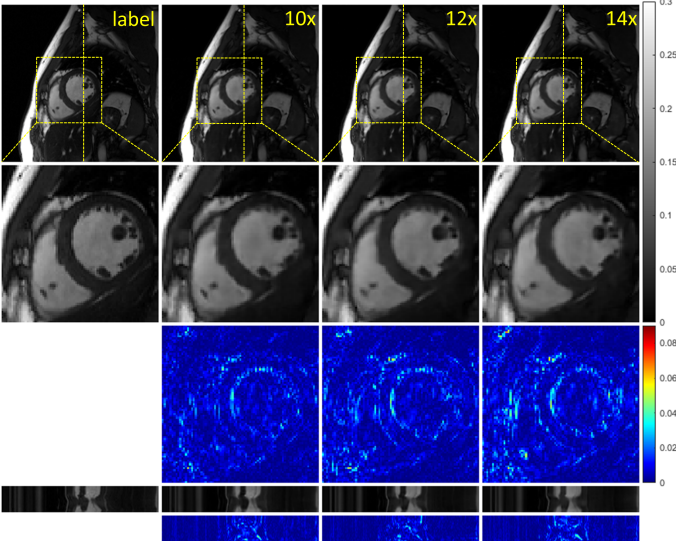


Fig. 3. The reconstruction results of the proposed PS-Net at 10-fold, 12-fold and 14-fold acceleration on a single-coil cardiac cine dataset. The first row shows the ground truth and the reconstruction results of these methods. The second row shows the enlarged views of their heart regions framed by a yellow box. The third row shows the error map (display range [0, 0.09]). The y-t image (extraction of the 92nd slice along the y and temporal dimensions) and the y-t image error are also given to show the reconstruction performance in the temporal dimension.

TABLE I
THE AVERAGE MSE, PSNR AND SSIM OF DIFFERENT METHODS AT 8-FOLD ON THE SINGLE-COIL CARDIAC CINE TEST DATASET (MEAN \pm STD)

AF	Methods	MSE(*e-5)	PSNR (dB)	SSIM(*e-2)
8×	L+S	8.48 \pm 2.03	40.83 \pm 1.00	95.53 \pm 0.89
	DC-CNN	6.02 \pm 1.06	42.28 \pm 0.83	96.64 \pm 0.47
	CRNN	4.52 \pm 0.68	43.49 \pm 0.70	97.44 \pm 0.28
	SLR-Net	3.90 \pm 1.37	44.37 \pm 1.60	97.83 \pm 0.56
	PS-Net	1.96 \pm 0.37	47.14 \pm 0.87	98.64 \pm 0.23

TABLE II
THE AVERAGE MSE, PSNR AND SSIM OF PS-Net AT 10-FOLD, 12-FOLD AND 14-FOLD ON THE SINGLE-COIL CARDIAC CINE TEST DATASET (MEAN \pm STD)

Methods	AF	MSE(*e-5)	PSNR (dB)	SSIM(*e-2)
PS-Net	10×	3.17 \pm 0.61	45.08 \pm 0.92	98.07 \pm 0.32
	12×	3.54 \pm 0.70	44.61 \pm 0.97	97.89 \pm 0.37
	14×	4.87 \pm 0.93	43.22 \pm 0.93	97.34 \pm 0.46

IV. CONCLUSION

In this paper, we proposed a model-based unrolled Partially Separable network, dubbed PS-Net, for dynamic MR reconstruction. In particular, we used the semi-quadratic splitting method to solve the optimization problem with the subspace and sparse regularization. Characterization of filter null space mapping was introduced to express low-rank more precisely. Then, the iterative steps were unrolled into a network whose regularization parameters are learnable. The proposed method was tested on a cardiac cine dataset. The experimental results showed that our method could improve the reconstruction results in both qualitative and quantitative metrics.

REFERENCES

- [1] B. Zhu, J. Z. Liu, S. F. Cauley, B. R. Rosen, and M. S. Rosen, “Image reconstruction by domain-transform manifold learning,” *Nature*, vol. 555, no. 7697, pp. 487–492, 2018.
- [2] S. Wang, Z. Su, L. Ying, X. Peng, S. Zhu, F. Liang, D. Feng, and D. Liang, “Accelerating magnetic resonance imaging via deep learning,” in *2016 IEEE 13th International Symposium on Biomedical Imaging*. IEEE, 2016, pp. 514–517.
- [3] K. Kwon, D. Kim, and H. Park, “A parallel mr imaging method using multilayer perceptron,” *Medical Physics*, vol. 44, no. 12, pp. 6209–6224, 2017.
- [4] Y. Han, J. Yoo, H. H. Kim, H. J. Shin, K. Sung, and J. C. Ye, “Deep learning with domain adaptation for accelerated projection-reconstruction mr,” *Magnetic Resonance in Medicine*, vol. 80, no. 3, pp. 1189–1205, 2018.
- [5] J. Schlemper, J. Caballero, J. V. Hajnal, A. N. Price, and D. Rueckert, “A deep cascade of convolutional neural networks for dynamic mr image reconstruction,” *IEEE Transactions on Medical Imaging*, vol. 37, no. 2, pp. 491–503, 2017.
- [6] C. Qin, J. Schlemper, J. Caballero, A. N. Price, J. V. Hajnal, and D. Rueckert, “Convolutional recurrent neural networks for dynamic mr image reconstruction,” *IEEE Transactions on Medical Imaging*, vol. 38, no. 1, pp. 280–290, 2018.
- [7] D. Liang, J. Cheng, Z. Ke, and L. Ying, “Deep magnetic resonance image reconstruction: Inverse problems meet neural networks,” *IEEE Signal Processing Magazine*, vol. 37, no. 1, pp. 141–151, 2020.
- [8] K. Hammernik, T. Klatzer, E. Kobler, M. P. Recht, D. K. Sodickson, T. Pock, and F. Knoll, “Learning a variational network for reconstruction of accelerated mri data,” *Magnetic Resonance in Medicine*, vol. 79, no. 6, pp. 3055–3071, 2018.
- [9] Y. Liu, Q. Liu, M. Zhang, Q. Yang, S. Wang, and D. Liang, “Ifr-net: Iterative feature refinement network for compressed sensing mri,” *IEEE Transactions on Computational Imaging*, vol. 6, pp. 434–446, 2019.
- [10] Z. Ramzi, G. Chaithya, J.-L. Starck, and P. Ciuci, “Nc-pdnet: a density-compensated unrolled network for 2d and 3d non-cartesian mri reconstruction,” *IEEE Transactions on Medical Imaging*, 2022.
- [11] T. Eo, Y. Jun, T. Kim, J. Jang, H.-J. Lee, and D. Hwang, “Kiki-net: cross-domain convolutional neural networks for reconstructing undersampled magnetic resonance images,” *Magnetic Resonance in medicine*, vol. 80, no. 5, pp. 2188–2201, 2018.
- [12] Z. Ke, W. Huang, Z.-X. Cui, J. Cheng, S. Jia, H. Wang, X. Liu, H. Zheng, L. Ying, Y. Zhu *et al.*, “Learned low-rank priors in dynamic mr imaging,” *IEEE Transactions on Medical Imaging*, vol. 40, no. 12, pp. 3698–3710, 2021.
- [13] W. Huang, Z. Ke, Z.-X. Cui, J. Cheng, Z. Qiu, S. Jia, L. Ying, Y. Zhu, and D. Liang, “Deep low-rank plus sparse network for dynamic mr imaging,” *Medical Image Analysis*, vol. 73, p. 102190, 2021.
- [14] J. Yoo, K. H. Jin, H. Gupta, J. Yerly, M. Stuber, and M. Unser, “Time-dependent deep image prior for dynamic mri,” *IEEE Transactions on Medical Imaging*, vol. 40, no. 12, pp. 3337–3348, 2021.
- [15] Z.-p. Liang, “Spatiotemporal imaging with partially separable functions,” in *2007 4th IEEE International Symposium on Biomedical Imaging*, 2007, pp. 988–991.
- [16] M. Vetterli, P. Marziliano, and T. Blu, “Sampling signals with finite rate of innovation,” *IEEE Transactions on Signal Processing*, vol. 50, no. 6, pp. 1417–1428, 2002.
- [17] A. Pramanik, H. K. Aggarwal, and M. Jacob, “Deep generalization of structured low-rank algorithms (deep-slrs),” *IEEE Transactions on Medical Imaging*, vol. 39, no. 12, pp. 4186–4197, 2020.
- [18] D. O. Walsh, A. F. Gmitro, and M. W. Marcellin, “Adaptive reconstruction of phased array mr imagery,” *Magnetic Resonance in Medicine*, vol. 43, no. 5, pp. 682–690, 2000.
- [19] H. Jung, J. C. Ye, and E. Y. Kim, “Improved k-t blast and k-t sense using focuss,” *Physics in Medicine & Biology*, vol. 52, no. 11, p. 3201, 2007.
- [20] X. Glorot, A. Bordes, and Y. Bengio, “Deep sparse rectifier neural networks,” in *Proceedings of the fourteenth international conference on artificial intelligence and statistics*, 2011, pp. 315–323.
- [21] M. Abadi, P. Barham, J. Chen, Z. Chen, A. Davis, J. Dean, M. Devin, S. Ghemawat, G. Irving, M. Isard *et al.*, “Tensorflow: A system for large-scale machine learning,” in *12th USENIX symposium on Operating Systems Design and Implementation (OSDI 16)*, 2016, pp. 265–283.
- [22] Z. Wang, A. C. Bovik, H. R. Sheikh, and E. P. Simoncelli, “Image quality assessment: from error visibility to structural similarity,” *IEEE Transactions on Image Processing*, vol. 13, no. 4, pp. 600–612, 2004.
- [23] R. Otazo, E. Candes, and D. K. Sodickson, “Low-rank plus sparse matrix decomposition for accelerated dynamic mri with separation of background and dynamic components,” *Magnetic Resonance in Medicine*, vol. 73, no. 3, pp. 1125–1136, 2015.
- [24] J. Schlemper, J. Caballero, J. V. Hajnal, A. N. Price, and D. Rueckert, “A deep cascade of convolutional neural networks for dynamic mr image reconstruction,” *IEEE Transactions on Medical Imaging*, vol. 37, no. 2, pp. 491–503, 2017.
- [25] C. Qin, J. Schlemper, J. Caballero, A. N. Price, J. V. Hajnal, and D. Rueckert, “Convolutional recurrent neural networks for dynamic mr image reconstruction,” *IEEE Transactions on Medical Imaging*, vol. 38, no. 1, pp. 280–290, 2018.